I.A. LYASHENKO, A.M. ZASKOKA

Sumy State University

(2, Rimskii-Korsakov Str., Sumy 40007, Ukraine; e-mail: nabla04@ukr.net, zaskoka23@ukr.net)

PACS 05.70.Ce; 05.70.Ln; 47.15.gm; 62.20.Qp; 64.60.-i; 68.35.Af; 68.60.-p

STICK-SLIP MODE OF BOUNDARY FRICTION AS THE FIRST-ORDER PHASE TRANSITION

A tribological system consisting of two contacting blocks has been considered. One of them is arranged between two springs, the other is driven periodically. The kinetics of the system has been studied in the boundary friction mode, when an ultrathin lubricant film is contained between the atomically smooth surfaces. In order to describe the film state, the expression for the free energy density is used in the form of an expansion in a power series in the order parameter, the latter being reduced to the shear modulus of a lubricant. The stick-slip mode is shown to be realized in a wide range of parameters, being a result of the periodic first-order phase transitions between kinetic friction regimes. The behavior of the system governed by internal and external parameters has been predicted.

K e y w o r d s: ultrathin lubricant film, boundary mode of friction, tribological system

1. Introduction

Owing to the rapid development of high-precision experimental techniques aimed at researching the nanosystems, the processes of friction in the case where the thickness of a lubricant between rubbing surfaces equals several atomic diameters have been intensively studied recently [1–3]. In tribology, this friction mode was called "boundary friction". It is often realized in ordinary mechanisms, because the rubbing surfaces contact with each other by means of surface irregularities or inhomogeneities [1, 4]. The boundary friction differs essentially from the hydrodynamic mode, when the friction force is proportional to a power function of the velocity. Note that the ultrathin film of a lubricant does not form conventional, thermodynamically equilibrium phases, solid and liquid ones. Instead, we have liquid- and solid-like states, which are kinetic friction modes, and there can be several of them [5, 6]. This occurs because the symmetry of a lubricant state is substantially affected by friction surfaces, this fact being not of importance for bulk lubricants. In the course of friction, the phase transitions of both the first and second orders can take place between the stationary states [7, 8]. These transitions often comprise the origin of the stick-slip motion mode for contacting surfaces [5, 6, 9].

In order to describe the boundary mode of friction and nano-contact phenomena, phenomenological models are widely used [7–10]. In particular, a model was developed [11], in which the lubricant melting is driven by the thermodynamic and shear mechanisms. In the framework of this model, the influence of additive fluctuations of principal quantities was studied [12], and their presence in the system was demonstrated to result in the emergence of new stationary states and new kinetic friction modes [13, 14], which are not essential for bulk systems. The origin of the hysteretic behavior, which was observed experimentally [3, 15, 16], was elucidated in work [17]. The indicated model also made it possible to describe the periodic stick-slip mode of motion [18, 19].

In works [7, 20], a thermodynamic scenario of boundary friction was proposed, which is based on the phase transition theory developed by Landau [21]. This model takes into account that the ultrathin film of a lubricant can melt and stay in a liquid-like disordered state both owing to the ordinary thermodynamic melting and as a result of overcoming the fluidity threshold by the shear stress component ("shear melting"). The influence of those factors was also studied in work [8], in which the excess volume [22, 23] arising owing to the lubricant stochastization at its melting was selected as the order parameter. As the excess volume increases, the shear

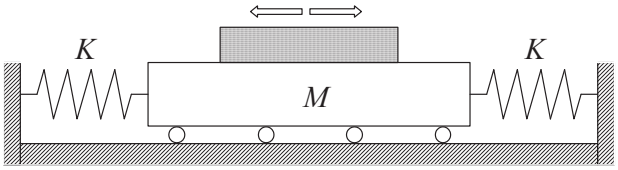

Fig. 1. Diagram of a tribological system

modulus decreases [8], which results in the melting. In works [7, 20], the shear modulus itself was selected as the order parameter, which acquires zero values in the liquid-like phase. However, in works [7, 20], the melting is described as a continuous phase transition of the second order, whereas jump-like phase transitions of the first order are often observed in the boundary friction mode [5, 6, 8], which are responsible for the stick-slip motion [5, 6].

This work is aimed at describing the first-order phase transition in the framework of the model developed in works [7, 20] and at studying the behavior of tribological systems on the basis of the indicated modification. The model proposed does not make allowance for specific types of lubricants, because its task consists in describing the origins of phenomena that take place at the boundary friction. For specific types of lubricants and friction surfaces, the model should be modified. To some extent, it can be made by choosing the numerical values of coefficients in the series expansions of the free energy, relaxation times, and so on. The model describes only homogeneous lubricants composed of non-polar quasispherical molecules [5, 6]. One of the reasons is the fact that we study a situation where the elastic stresses acquire zero values in the liquid-like state, i.e. the melting gives rise to the total disordering of lubricant molecules, which does not takes place in thin lubricant films consisting of polymer molecules. Another reason is the fact that the obtained time dependences of the friction force and stresses are strictly periodic, which is also observed for quasispherical molecules only [5, 6].

2. Tribological System

The fabrication of atomically smooth surfaces with large dimensions is associated with considerable technological difficulties. Therefore, to measure the dynamic parameters of ultrathin lubricant films between such surfaces, the surfaces characterized by small dimensions and pasted on spherical or cylindrical surfaces that rub each other are used. This scheme was applied while designing the surface force apparatus (SFA) [3, 24, 25]. Two types of SFA—Mk II and Mk III—were described in review [3]. In the latter, the system to control distances between rubbing surfaces was improved. The device allows the shape of surfaces to be determined, as well as the distance between them to within an accuracy of 1 Å. The contact area between surfaces is measured with an accuracy of $\pm 5\%$, the normal and shear components of operating forces to within $\pm 1\%$, and the magnitude of applied loading to within $\pm 5\%$.

One of the rubbing surfaces in the SFA is fixed, and the other is driven to move periodically. In the course of motion, the shear stresses and the effective viscosity of a lubricant are measured, the lubricant structure is determined, and so forth. In this work, we consider a simplified mechanical analog of the SFA exhibited in Fig. 1. Two springs characterized by the stiffness constant K are connected with a block of mass M mounted on rollers. The rolling friction for the latter is neglected below. On the indicated block, another block is arranged, which is brought into a periodic motion by applying an external force. Provided that the surfaces of two blocks interact with each other, the motion of the upper block stimulates the motion of the lower one. The trajectory of the lower block substantially depends on the friction mode established in the system. A similar tribological system was experimentally studied in works [26, 27]. Note that, in contrast to the SFA design, now both blocks are mobile, which enables the time dependences of block coordinates and velocities to be registered, and, by analyzing them, the rheological and tribological characteristics of the system to be determined.

Let X and $V = \dot{X}$ be the coordinate and the velocity, respectively, of the upper block, whereas x and $v = \dot{x}$ denote the corresponding quantities for the lower block. Let us consider the case where the upper block moves according to the cyclic law,

$$X = X_m \cos \omega t, \tag{1}$$

$$V = -X_m \omega \sin \omega t, \tag{2}$$

where X_m is the amplitude, and ω is the cyclic frequency. We write down the equation of motion for the lower block in the form [26]

$$M\ddot{x} + 2Kx - F = 0, \tag{3}$$

where F is the friction force that arises between the blocks at their relative motion. From the last expression, it follows that the character of motion in the

system essentially depends on the friction mode and the lubricant properties, because they determine the force F.

The friction force is determined in a standard way,

$$F = \sigma A, \tag{4}$$

where σ is the shear stress that arises in the lubricant, and A is the contact area between rubbing surfaces.

In the boundary friction mode, the elastic, $\sigma_{\rm el}$, and viscous (dissipative), σ_v, stresses arise in the lubricant layer [7, 8, 16]. As a rule, the melting is accompanied by a reduction of the elastic stress component, whereas the viscous one grows owing to an increase of the relative shear velocity between rubbing surfaces [16]. Hence, the total stress is determined by the sum of indicated components,

$$\sigma = \sigma_{\rm el} + \sigma_v. \tag{5}$$

The viscous stresses in the lubricant layer are determined by the empirical formula [28, 29]

$$\sigma_v = \frac{\eta_{\rm eff}(V - v)}{h}, \tag{6}$$

where the effective viscosity of the lubricant, $\eta_{\rm eff}$ (it depends on plenty of factors and is determined experimentally) is introduced into consideration, as well as the relative velocity of surface motion, $V - v$.

As a result, in the case of boundary friction, polymer solutions or melts are applied as lubricants. The necessity of such an application is caused by the fact that the friction surfaces are small in dimensions, and the lubricant film between them must not be squeezed out under the influence of large tribological loadings. Such lubricants are non-Newtonian fluids, the viscosity of which depends not only on the temperature, but also on the velocity gradient. However, the application of the SFA allows the behavior of a wide class of lubricants to be examined in the boundary friction mode, because the rubbing surfaces in these experiments are completely imbedded into a vessel with a liquid to study, so that the latter is not squeezed out from the gap between the surfaces during their motion [3]. However, we should note that even ordinary water, when being used as a boundary lubricant, can behave as a non-Newtonian fluid, because, owing to its interaction with the surfaces, it can create spatially ordered structures in the course of motion.

The non-Newtonian fluids are divided into two classes: pseudoplastic fluids, the viscosity of which decreases with the growth of the strain rate (e.g., these are polymer solutions and melts) and dilatant ones, the viscosity of which increases as $\dot{\varepsilon}$ grows (e.g., suspensions of solid particles). For both situations to be taken into account, let us use a simple power-law approximation [28, 29]

$$\eta_{\rm eff} = k(\dot{\varepsilon})^{\gamma}. \tag{7}$$

Here, we introduced the proportionality coefficient k (its dimension is $\mathrm{Pa} \cdot \mathrm{s}^{\gamma+1}$) and the dimensionless index γ (for pseudoplastic fluids, $\gamma < 0$; dilatant ones are characterized by the index $\gamma > 0$; and $\gamma = 0$ in the case of Newtonian fluids).

The strain rate is determined through the relative velocity of motion and the lubricant thickness h [28],

$$\dot{\varepsilon} = \frac{V - v}{h}. \tag{8}$$

Taking Eqs. (7) and (8) into account, the expression for viscous stresses (Eq. (6)) looks like

$$\sigma_v = k \left(\frac{V - v}{h}\right)^{\gamma+1}. \tag{9}$$

Note that, according to Eq. (9), viscous stresses are available in both the liquid- and solid-like states of a lubricant. The presence of viscous (dissipative) stresses in both phases was indicated in the experimental work [16]. However, if the lubricant is in a solid-like state, viscous stresses are low, because, in accordance with Eq. (9), they are proportional to the relative shear velocity, $V - v$, which is low in this case.

Substituting Eqs. (5) and (9) into Eq. (4), we obtain the final expression for the friction force [30–33],

$$F = \left[\sigma_{\rm el} + k\ \mathrm{sgn}(V - v) \left(\frac{|V - v|}{h}\right)^{\gamma+1}\right] A, \tag{10}$$

where the function

$$\mathrm{sgn}(V - v) = \begin{cases} 1, & V \geq v, \\ -1, & V < v \end{cases} \tag{11}$$

takes into account the direction of force action. The first term in Eq. (10) describes the elastic component of the friction force, and the second is responsible for the viscous one, which grows with the velocity. Hence, the friction force depends on the velocity of the lower block, v, and the elastic stresses, $\sigma_{\rm el}$, that arise in a lubricant.

3. Thermodynamic Model

In the homogeneous case, the free energy density for an ultrathin lubricant layer looks like [7, 20, 30, 31]

$$f = \alpha(T - T_c)\varphi^2 + \frac{a}{2}\varphi^2\varepsilon_{\rm el}^2 - \frac{b}{3}\varphi^3 + \frac{c}{4}\varphi^4, \qquad (12)$$

where T is the lubricant temperature; T_c is the critical temperature; $\varepsilon_{\rm el}$ is the shear component of the elastic strain; α, a, b, and c are positive constants, and φ is the order parameter (the amplitude of the periodic component in the microscopic medium density function [7, 20]). The parameter φ equals zero in the liquid-like phase and acquires nonzero values in the solid-like one. In comparison with works [7, 20], potential (12) takes additionally the third-order term into account. This form of expansion is used to describe phase transitions of the first order [21, 34]. In the second term in Eq. (12), we also introduced the factor a, which allows us to vary the contribution of the elastic energy to the potential.

The elastic stresses that arise in the lubricant layer, according to Eq. (12), are determined as the derivative $\sigma_{\rm el} = \partial f/\partial\varepsilon_{\rm el}$, so that

$$\sigma_{\rm el} = a\varphi^2\varepsilon_{\rm el}. \qquad (13)$$

Therefore, after the coefficient a has been introduced into expansion (12), the shear modulus is determined as follows:

$$\mu = a\varphi^2. \qquad (14)$$

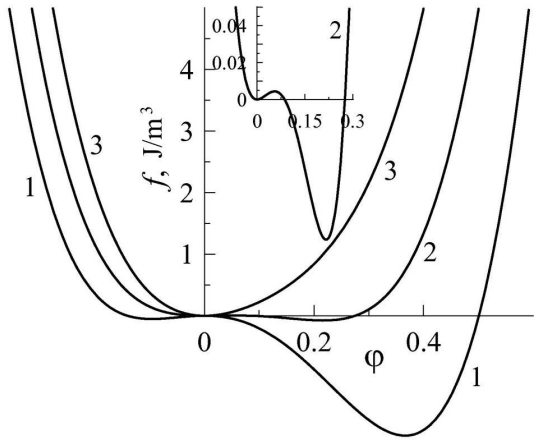

Fig. 2. Dependences of the free energy density f (see Eq. (12)) on the dimensionless order parameter φ for various temperatures T = 265, 286, and 310 K (curves *1* to *3*, respectively). The calculation parameters are $\alpha = 0.95$ J/(K · m^3), $T_c = 290$ K, $a = 4 \times 10^{12}$ Pa, $b = 230$ J/m^3, $c = 850$ J/m^3, and the shear strain $\varepsilon_{\rm el} = 2.1 \times 10^{-6}$

Depending on the value of parameter a, it can acquire both small and large values at $|\varphi| < 1$. Note that, in the boundary friction mode, the shear modulus can be several orders of magnitude larger than that in the hydrodynamic mode for the same lubricant. As a result, if the critical temperature T or critical elastic shear stress $\sigma_{\rm el}$ become exceeded in the course of friction, the lubricant does not melt completely; instead, a domain structure with regions of liquid-assisted and dry friction is created. For this situation to be studied, Eq. (12) must include gradient terms, which considerably complicates the subsequent consideration. However, the examination of such spatial structures comprises a separate problem, which is not the purpose of this work. Therefore, the gradient terms are excluded from Eq. (12), which corresponds to the consideration of a lubricant behavior in the framework of the one-domain model with a homogeneous structure.

According to the principle of minimum energy, the system tends to occupy a stationary state, which corresponds to the minimum of the free energy $f(\varphi)$ (see Eq. (12)), irrespective of its initial conditions. Since the parameter φ is the amplitude of the periodic component in the microscopic medium density function, we consider below only the physical range of values $\varphi \geq 0$. Let us introduce the function

$$B(\varepsilon_{\rm el}, T) = a\varepsilon_{\rm el}^2 + 2\alpha(T - T_c). \qquad (15)$$

The analysis of expression (12) for the free energy allows the following situations to be distinguished. Provided that the condition $B(\varepsilon_{\rm el}, T) \leq 0$ is obeyed, the maximum of potential (12) at $\varphi = 0$ and its minimum at $\varphi > 0$ are realized (curve *1* in Fig. 2). In this case, the lubricant is solid-like, because the shear modulus $\mu > 0$. In the intermediate interval $0 < B(\varepsilon_{\rm el}, T) < b^2/(4c)$, the maximum of the potential at $\varphi = 0$ transforms into a minimum and, additionally, there emerges a maximum that separates the zero and nonzero minima (curve *2* in Fig. 2; it is also shown scaled-up in the inset). In this case, the state of a lubricant depends on the initial conditions, and the lubricant can be in either solid- or liquid-like state. In the latter case, $B(\varepsilon_{\rm el}, T) \geq b^2/(4c)$, and a single minimum of the potential at $\varphi = 0$ is realized (curve *3* in Fig. 2), which, according to Eq. (14), corresponds to the zero value of lubricant shear modulus and its liquid-like structure.

The stationary values of order parameter φ are determined as the roots of the equation $\partial f/\partial\varphi = 0$

[30, 31], namely,

$$\varphi_{\mp} = \frac{b}{2c} \mp \sqrt{\left(\frac{b}{2c}\right)^2 - \left(\frac{a}{c}\varepsilon_{\rm el}^2 + \frac{2\alpha(T-T_c)}{c}\right)}. \quad (16)$$

The root φ_- is related to the unstable stationary state, because it corresponds to the maximum of potential (12). The stable state, which corresponds to the potential minimum, is given by the root φ_+. Besides roots (16), the stationary solution $\varphi_0 = 0$ always exists, which corresponds to the extremum of potential (12) with the order parameter equal to zero; it can be either a maximum or minimum of the potential. According to Eq. (16), the lubricant melts if either the temperature T elevates or the shear component of the elastic strain, $\varepsilon_{\rm el}$, grows. Thus, the model concerned makes allowance for both thermodynamic and shear meltings.

As was already indicated above, at small values of temperature T and strain $\varepsilon_{\rm el}$, when the function $B(\varepsilon_{\rm el}, T) \le 0$, the lubricant is solid-like, because, in accordance with Eq. (16), a stationary value of parameter φ different from zero is realized, and, according to Eq. (14), the shear modulus μ is also non-zero. In this case, the potential has a single minimum at $\varphi \ge 0$. If the temperature T exceeds the critical value

$$T_{c0} = T_c - \frac{a}{2\alpha}\varepsilon_{\rm el}^2 + \frac{b^2}{8\alpha c}, \quad (17)$$

the order parameter vanishes in a jump-like manner, when the lubricant passes into the liquid-like state, in which the potential $f(\varphi)$ has a single minimum at $\varphi = 0$ [30, 31]. If, after this transition, the temperature T falls down further, the lubricant solidifies following the mechanism of first-order phase transformation at a lower temperature,

$$T_c^0 = T_c - \frac{a}{2\alpha}\varepsilon_{\rm el}^2, \quad (18)$$

and the parameter φ becomes non-zero again. In the intermediate temperature region, $T_c^0 < T < T_{c0}$, the potential is characterized by two minima at positive φ. Hence, the dependence $\varphi(T)$ has a hysteresis character [30, 31] and corresponds to the phase transition of the first order. Expression (18) elucidates the physical meaning of the critical temperature T_c; namely, it is the temperature of lubricant solidification at zero strains, when only the mechanism of thermodynamic melting is active in the system.

From expression (17), it follows that the lubricant melts not only at the temperature elevation, but also if it is subjected to an external mechanical action, when the elastic strain component exceeds the critical value

$$\varepsilon_{{\rm el},c0} = \sqrt{\frac{2\alpha(T_c - T)}{a} + \frac{b^2}{4ac}}. \quad (19)$$

Using formula (18), we can determine the elastic deformation $\varepsilon_{\rm el}$, at which the lubricant solidifies,

$$\varepsilon_{{\rm el},c}^0 = \sqrt{\frac{2\alpha(T_c - T)}{a}}. \quad (20)$$

Note that, according to relation (19), the melting can occur even at the zero temperature, $T = 0$, if the strain exceeds the critical value. At the zero strain, i.e. at $\varepsilon_{\rm el} = 0$, the lubricant melts, when its temperature exceeds the critical value T_{c0} (see Eq. (17)).

As a rule, it is the relative shear velocity between friction surfaces rather than the shear strain component $\varepsilon_{\rm el}$ that is registered in experiments [5,6]. Therefore, for our research to go further, it is necessary to obtain a relation between those two quantities. Let us take advantage of the Debye approximation, according to which the elastic strain component $\varepsilon_{\rm el}$ arises in the lubricant layer, when the latter flows plastically at the velocity [7]

$$\dot{\varepsilon}_{\rm pl} = \frac{\varepsilon_{\rm el}}{\tau_\varepsilon}, \quad (21)$$

where τ_ε is the Maxwell relaxation time for internal stresses. The total strain in the layer is determined as the sum of elastic, $\varepsilon_{\rm el}$, and plastic, $\varepsilon_{\rm pl}$, components [7, 23]

$$\varepsilon = \varepsilon_{\rm el} + \varepsilon_{\rm pl}. \quad (22)$$

Combining relations (8), (21), and (22), we obtain the kinetic equation for the evolution of the elastic component of the shear strain [8, 30, 31, 33]:

$$\tau_\varepsilon \dot{\varepsilon}_{\rm el} = -\varepsilon_{\rm el} + \frac{(V-v)\tau_\varepsilon}{h}. \quad (23)$$

Boundary friction experiments testify that the relaxation time of the elastic strain is very short, as a rule. This quantity can be estimated from the relation $\tau_\varepsilon \approx a/c \sim 10^{-12}$ s, where $a \sim 1$ nm is the lattice constant or the intermolecular distance, and $c \sim 10^3$ m/s is the sound velocity [11]. However, in the boundary mode, the strain relaxation time, τ_ε, can differ by several orders of magnitude [5, 6]. Bearing in mind that the value of strain relaxation time τ_ε is small, below

we use the adiabatic approximation $\tau_\varepsilon \dot{\varepsilon}_{\rm el} \approx 0$ [35], which allows us to determine the strain by its stationary value

$$\varepsilon_{\rm el}^0 = \frac{(V-v)\tau_\varepsilon}{h}, \tag{24}$$

rather than by Eq. (23).

In the general case, the free energy (12) depends on the lubricant layer thickness h [20]. Note that, in the framework of our model, the second term in expression (12) is proportional to the square of the elastic strain, $\varepsilon_{\rm el}^2$. In accordance with relation (24), the stationary elastic strain increases with a reduction of the lubricant thickness h. Therefore, in the limiting case of a very thin layer ($h \to 0$), the strain $\varepsilon_{\rm el} \to \infty$. In this case, the second term in expansion (12) dominates, and the stationary value of order parameter equals zero, so that the lubricant is liquid-like, as in work [20]. A detailed study of the influence of the lubricant layer thickness on friction modes was carried out in works [36, 37].

4. Kinetics of Melting

The changes in the lubricant temperature T and the strain $\varepsilon_{\rm el}$ induce variations of the order parameter φ, which governs the free energy f (see Eq. (12)) in accordance with the power-law expansion of the latter [21]. The stabilization time for a new stationary value φ_+ (see Eq. (16)) is determined by the generalized thermodynamic force $-\partial f/\partial\varphi$. If $\varphi \approx \varphi_+$, this force is small, and the relaxation process is described by the Landau–Khalatnikov linear kinetic equation [38]

$$\dot{\varphi} = -\delta \frac{\partial f}{\partial \varphi}, \tag{25}$$

where the kinetic coefficient δ characterizes the inertial properties of the system. After substituting energy (12) into Eq. (25), we obtain the equation in the explicit form,

$$\dot{\varphi} = -\delta \left(2\alpha(T-T_c)\varphi + a\varphi\varepsilon_{\rm el}^2 - b\varphi^2 + c\varphi^3\right) + \xi(t). \tag{26}$$

Equation (26) includes a term responsible for additive fluctuations with a low intensity [30, 31]. Their intensity is selected to be so low that they do not affect the deterministic behavior of the system. However, their introduction is necessary, because, at subsequent numerical calculations, the root $\varphi = 0$ of Eq. (26) corresponding to the maximum of the potential $f(\varphi)$, i.e. to the unstable stationary state, turns out stable according to the structure of the equation. In this situation, the introduction of $\xi(t)$ stimulates the system to transit from the unstable state into a stable one, which corresponds to the energy minimum. Hence, fluctuations are taken into consideration by means of the features in subsequent numerical calculations.

The dynamic characteristics of any tribological system are governed by its properties in whole. For instance, in the geometry illustrated in Fig. 1, the behavior of the system substantially depends on the stiffness constant, K, of the spring and the mass of the lower block, M. In contrast to the case of motion with constant elastic strains, this tribological system can reveal the stick-slip mode of motion in the course of friction [5, 6, 9, 18]. The indicated mode is established because the lubricant periodically melts and solidifies in the course of motion, which leads to the oscillatory character of friction force F. To calculate the evolution of this system in time, we need to solve the system of kinetic equations (3) and (26) numerically, determining the friction force F from Eqs. (10) and (11), the elastic stresses $\sigma_{\rm el}$ from Eq. (13), and the strain $\varepsilon_{\rm el}$ from relation (24). In so doing, we have to take into account the relation $\dot{x} = v$, as well as definitions (1) and (2).

While solving the differential equations numerically, we used the Euler–Cramer method with the time increment $\Delta t = 10^{-10}$ s. The initial conditions $\varphi_0 = x_0 = v_0 = 0$ were chosen. The result obtained is shown in Fig. 3. The dashed curve in the upper panel corresponds to the time dependence of the upper block coordinate $X(t)$ (see Eq. (1)), and the solid one to that of the lower block, $x(t)$, which is more complicated. The figure also exhibits the time dependences for the block velocities, elastic shear stresses $\sigma_{\rm el}$ (see Eq. (13)) that arise in the lubricant, and total friction force F (see Eq. (10)). Let us examine these dependences in more details.

At the initial time moment, $t = 0$, the blocks are motionless, and the lubricant is in the solid-like state, because the dependences are plotted for the lubricant temperature T lower than the critical one, T_c^0 (see Eq. (18)), and $\varepsilon_{\rm el} = 0$ at rest. At $t = 0$, the upper block starts to move, and, at $t > 0$, its velocity grows in accordance with Eq. (2). Since the lubricant is in the solid-like state, the friction force F possesses both the viscous and elastic components, and the lower block moves together with the upper one. However,

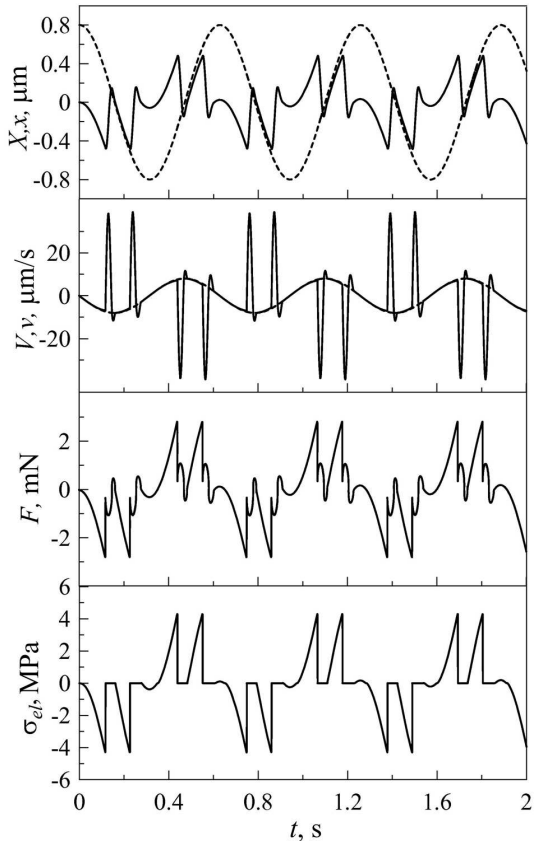

Fig. 3. Dependences of the coordinates X and x, the velocities V and v, the elastic stresses $\sigma_{\rm el}$ (see Eq. (13)), and the friction force F (see Eq. (10)) on the time t for the same parameters as in Fig. 2 and $h = 10^{-9}$ m, $\tau_\varepsilon = 10^{-8}$ s, $\gamma = -2/3$, $A = 0.6 \times 10^{-9}$ m^2, $k = 5 \times 10^4$ Pa $\cdot$ s$^{1/3}$, $\delta = 100$ m^3/(J $\cdot$ s), $T = 200$ K, $X_m = 0.8 \times 10^{-6}$ m, $\omega = 10$ rad/s, $M = 0.4$ kg, and $K = 3000$ N/m. The dashed curves correspond to the coordinate $X(t)$ and the velocity $V(t)$ of the upper block, and the solid ones to the coordinate $x(t)$ and the velocity $v(t)$ of the lower block

in the course of motion, the absolute value of elastic force $2Kx$, which impedes the lower block to move, grows and, as a result, the velocity v does not increase so sharply as the velocity V does. Hence, the relative shear velocity between block surfaces, $V-v$, increases in time and, in accordance with Eq. (24), the elastic strain $\varepsilon_{\rm el}$ also grows. At a certain time moment, the condition $\varepsilon_{\rm el} > \varepsilon_{{\rm el},c0}$ (see Eq. (19)) becomes satisfied, and the lubricant begins to melt following the "shear melting" mechanism. The friction force substantially decreases at that, because the stresses vanish, and the lower block can slide for a considerable distance, being driven by the elastic force from the compressed and stretched springs. Therefore, the relative shear

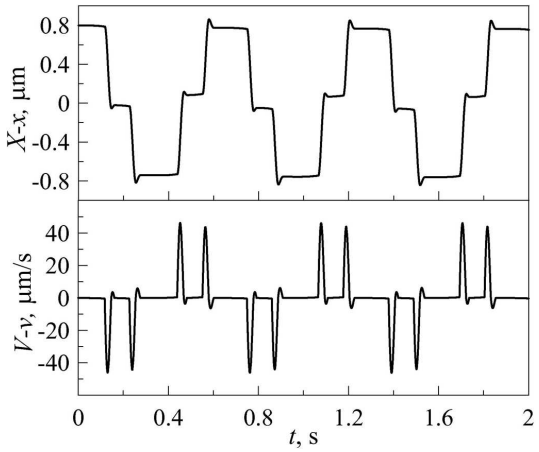

Fig. 4. Dependences of the relative displacement, $X - x$, and the velocity, $V - v$, of blocks on the time t for the same parameters as in Fig. 3

velocity diminishes, and, when the condition $\varepsilon_{\rm el} < \varepsilon^0_{{\rm el},c}$ (see Eq. (20)) is obeyed, the lubricant solidifies again. The considered process repeats periodically.

In addition, Fig. 4 demonstrates the time dependences of the relative block displacement and the velocity. At the time moments, when the surfaces "stick" to each other, their relative displacement $X-x$ remains constant, and the relative shear velocity $V-v$ is close to zero (in this case, the dependences $V(t)$ and $v(t)$ in Fig. 3 visually coincide). Hence, the periodic stick-slip mode of motion takes place, which is also typical of dry friction, when no lubricant is used [1, 2, 39]. For the chosen parameter values, the blocks "stick" to each other four times during a complete period of parameter changes: two times in each direction of motion, with the obtained dependences being symmetric with respect to the motion direction. However, a number of different situations can be realized depending on the system parameters.

The phase portraits of the system calculated at the same parameters as in Fig. 3 and various values of cyclic frequency ω are depicted in Fig. 5. The kinetic dependences in Fig. 3 completely correspond to the phase portrait in Fig. 5,*a*, because they were calculated for the same frequency ω value. It is important to emphasize the fact that the phase portraits in Figs. 5,*a* and *c* are symmetric with respect to the coordinate origin, whereas the phase portraits in Fig. 5,*b* and *d* illustrate the situation where the motion of the upper friction surface in one direction affects differently the motion of the lower block in comparison with its motion in the opposite direction. Hence, the system reveals memory effects, which were

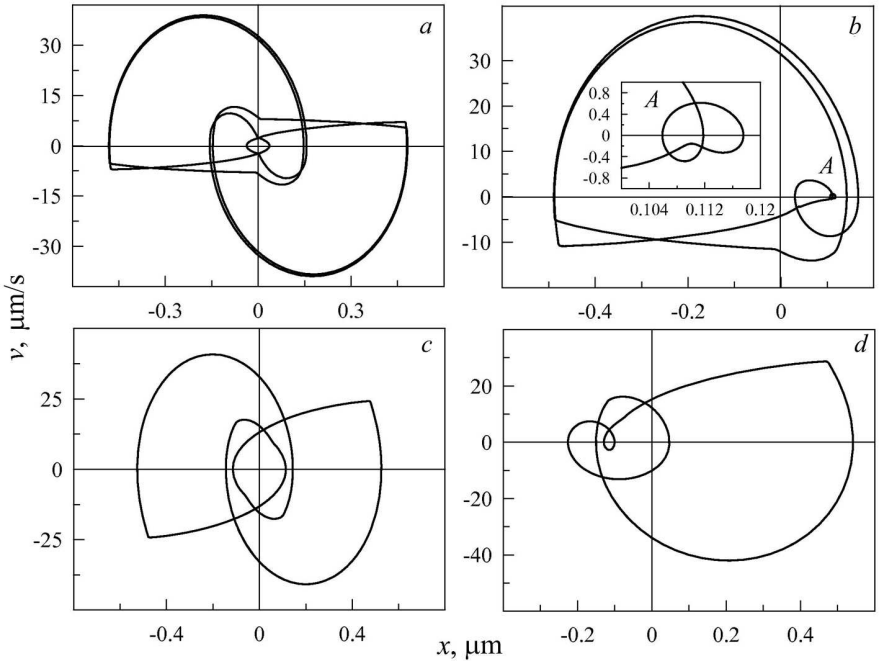

Fig. 5. Phase portraits of the system at the same parameters as in Fig. 3 and various values of the cyclic frequency $\omega = 10$ (a), 15 (b), 32 (c), and 38 rad/s (d)

observed experimentally [5]. In this case, the motion of the lower block is also periodic in time, but the time dependences of the parameters, which are given in Fig. 3, are not symmetric with respect to their zero values [30]. The inset in Fig. 5,b demonstrates the enlarged section conditionally marked by letter A, because this section has pronounced features, which cannot be distinguished in the main plot. Thus, the frequency ω affects the behavior of the tribological system in a non-trivial manner. By varying ω, it is possible to select various modes of motion, which considerably differ from one another. Note that, at some frequencies, the stationary behavior of the system, which is established as a result of the system evolution, depends on the initial conditions or the system prehistory. For instance, in Fig. 5,d, the initial value $\varphi_0 \neq 0$ gives rise to a mode similar to that exhibited in Fig. 5,c. This circumstance also confirms the presence of memory effects in the system, which were observed experimentally [5].

Figure 6 elucidates the influence of lubricant temperature T on the melting kinetics. The plotted dependences are divided into four sections. The temperature for the first section is the lowest, and, for every next section, the temperature increases, i.e. we have the inequalities $T_1 < T_2 < T_3 < T_4$. The dependence obtained in the first section, at $T = T_1$, reproduces the dependence shown in Fig. 3 in more details, because it was obtained at the same T-value. As the temperature is elevated to $T = T_2$, the stick-slip mode of motion is realized, as it was at $T = T_1$. However, the maximum value of elastic stresses $\sigma_{\rm el}$ decreases at $T = T_2$. As a result, the friction force F in the solid-like lubricant also decreases, as the temperature grows. As the temperature is elevated to $T = T_3$, this tendency survives. Note that a reduction of the sticking peak number with the temperature growth is not a rule, and the opposite situation can take place. At $T = T_4$, the lubricant is liquid-like all the time, and the elastic stresses equal zero. It is so, because, at this temperature, the condition $T > T_c^0$ (see Eq. (18)) is obeyed even if $\varepsilon_{\rm el} = 0$, i.e. the melted lubricant cannot solidify due to a reduction of the relative shear velocity between the rubbing surfaces. We do not know of any experiments devoted to similar researches of the influence of the temperature on the friction mode. Therefore, the dependences exhibited in Fig. 6 are a forecast.

5. Numerical Experiment

The dependences shown in Fig. 6 testify that the growth of the temperature T gives rise to a reduction of the elastic stress amplitude $\sigma_{\rm el}$ and a reduction of the friction force F maximum. Let is ana-

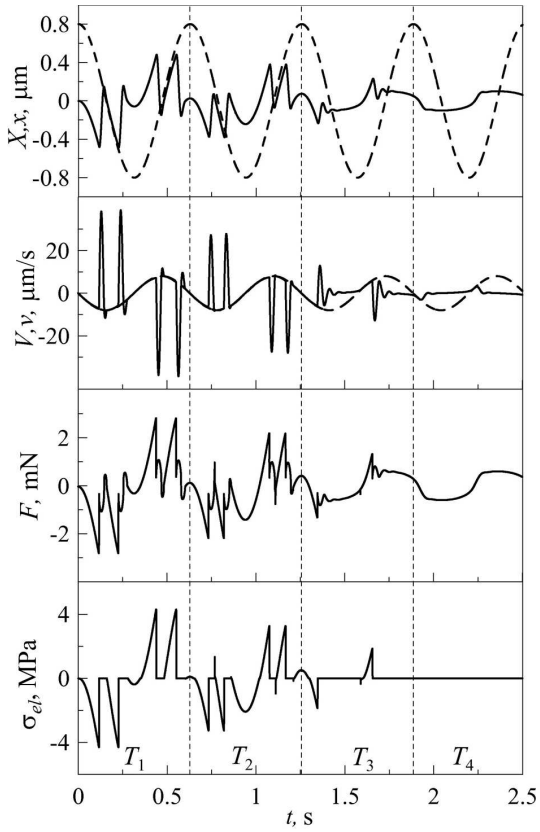

Fig. 6. Dependences of the coordinates X and x, the velocities V and v, the elastic stresses $\sigma_{\rm el}$ (see Eq. (13)), and the friction force F (see Eq. (10)) on the time t for the same parameters as in Fig. 3 and the temperatures $T_1 = 200$ K, $T_2 = 220$ K, $T_3 = 250$ K, and $T_4 = 300$ K.The dashed curves correspond to the $X(t)$ and $V(t)$ dependences, and the solid curves to the $x(t)$ and $v(t)$ ones

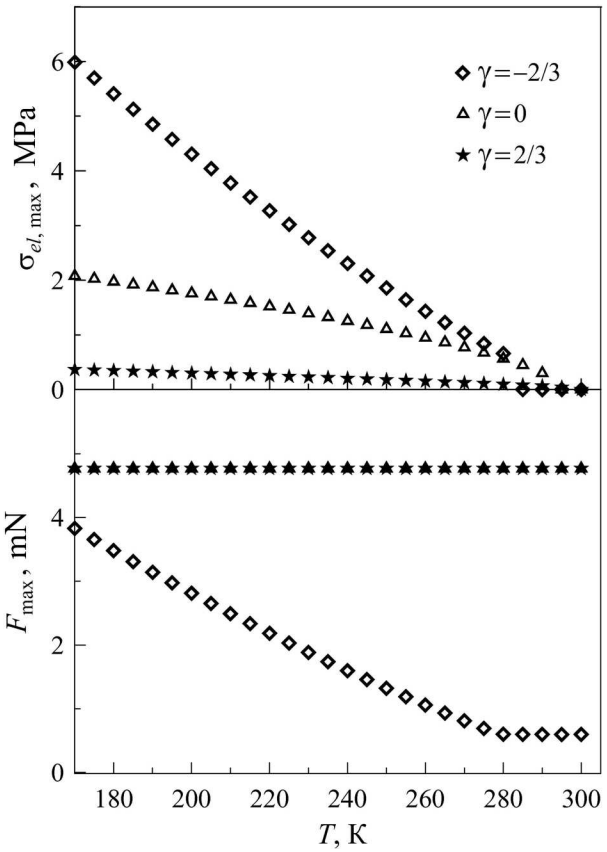

Fig. 7. Dependences of the elastic stress, $\sigma_{\rm el,max}$, and friction force, $F_{\rm max}$, amplitudes on the temperature T for pseudoplastic ($\gamma = -2/3$), Newtonian ($\gamma = 0$), and dilatant ($\gamma = 2/3$) fluids as a lubricant. The parameters are the same as in Fig. 3

lyze the dependences of the $\sigma_{\rm el}$ and F amplitudes on the temperature T at various modes of functioning of the system in more details. We define the stress amplitude as $\sigma_{\rm el,max} := (\sigma_{\rm el,max} - \sigma_{\rm el,min})/2$ and the friction force amplitude as $F_{\rm max} := (F_{\rm max} - F_{\rm min})/2$, where $\sigma_{\rm el,max}$ and $F_{\rm max}$ are the maximum values of elastic stresses and friction force, respectively, and $\sigma_{\rm el,min}$ and $F_{\rm min}$ are their minimum values, which are determined within the complete period of parameter changes, $T = 2\pi/\omega$, after the stationary friction mode has been established.

The dependences of the indicated quantities on the temperature are depicted in Fig. 7 for three types of lubricants: pseudoplastic ($\gamma < 0$), Newtonian ($\gamma = 0$), and dilatant ($\gamma > 0$) fluids. The upper panel demonstrates that, as the temperature increases, the elastic stresses $\sigma_{\rm el,max}$ decrease for all three types of fluids, i.e. the temperature elevation favors the lubricant melting. Note that, for pseudoplastic fluids ($\gamma = -2/3$), which are used most often as lubricants in such systems, the stress amplitude attains maximum values within almost the whole presented range of temperatures, but the melting occurs at lower T in this case. The lower panel of the figure shows the dependences of the friction force amplitudes $F_{\rm max}$ on the lubricant temperature T. It follows from the figure that the friction force decreases with the temperature growth only for pseudoplastic fluids, and it is minimal within the whole range of temperatures in comparison with other types of fluids. For dilatant and Newtonian fluids and for the selected parameter values, the maximum friction force does not change with the temperature growth. Since the elastic stresses for those fluids decrease as the temperature grows (the upper panel of the figure), this means that the growth of T gives rise to an increase of the viscous component of the friction force, to which the second term in

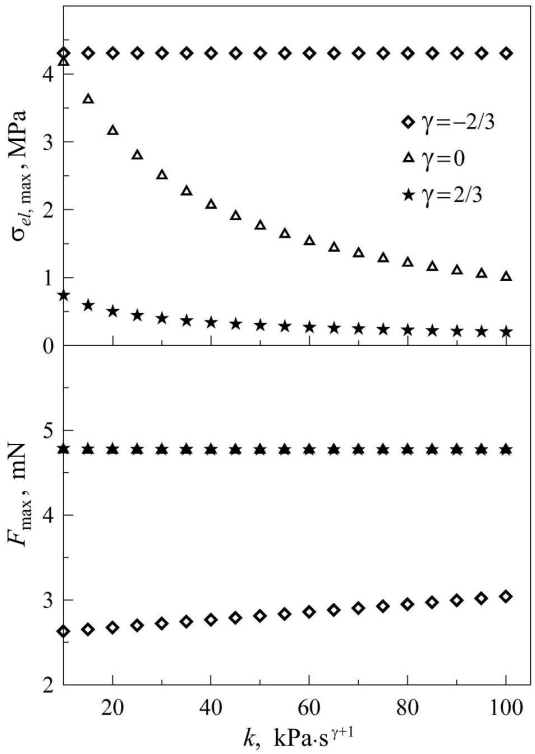

Fig. 8. Dependences of the elastic stress, $\sigma_{\mathrm{el,max}}$, and friction force, F_{max}, amplitudes on the proportionality coefficient k (see Eq. (7)) for pseudoplastic ($\gamma = -2/3$), Newtonian ($\gamma = 0$), and dilatant ($\gamma = 2/3$) fluids as a lubricant. The parameters are the same as in Fig. 3

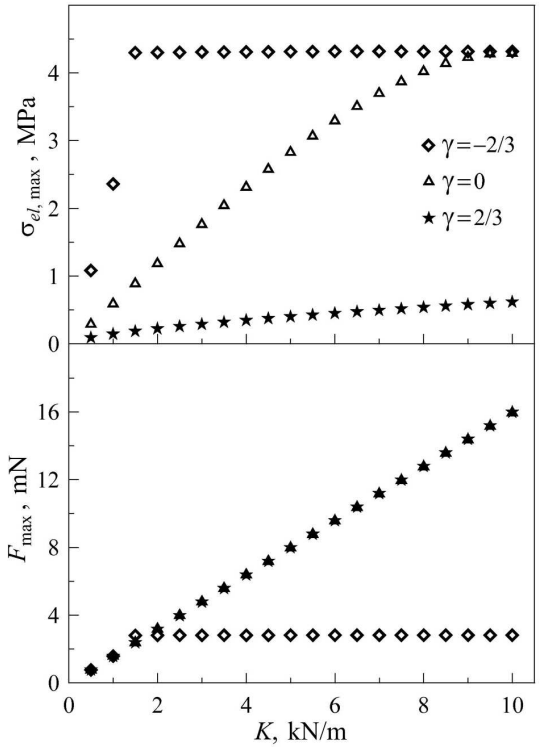

Fig. 9. Dependences of the elastic stress, $\sigma_{\mathrm{el,max}}$, and friction force, F_{max}, amplitudes on the spring stiffness constant K (see Eq. (3)) for pseudoplastic ($\gamma = -2/3$), Newtonian ($\gamma = 0$), and dilatant ($\gamma = 2/3$) fluids as a lubricant. The parameters are the same as in Fig. 3

formula (10) corresponds. In the situation concerned, this can happen only if the relative velocity of motion, $V - v$, increases. Note that, according to the figure, the amplitude of the friction force for the Newtonian and dilatant fluids remains constant when the temperature grows, even in the case $\sigma_{\mathrm{el}} = 0$, i.e. when the friction force has only the viscous component. Since the F-amplitudes in the cases $\gamma = 0$ and $\gamma = 2/3$ coincide at all temperatures, it is not sufficient to experimentally measure the total friction force in order to determine the friction mode. That is why the behavior of the elastic, σ_{el}, and viscous, σ_v, stresses are additionally studied as a rule [16]. Note also that, according to the results demonstrated in Fig. 7, the application of pseudoplastic fluids is optimal to reduce friction, because they favor the establishment of a mode with minimum force F, despite that the elastic stresses for such lubricants are maximum within almost the whole range of temperatures.

To determine the dependence of the viscosity on the velocity gradient and the temperature, both real [28] and computer-assisted [29] experiments are carried out. The problem urgency is connected with the fact that the dependences of the viscosity on the indicated quantities are anomalous in the boundary friction mode in the case of nano-sized tribological systems. There can even be a mode, when the friction force almost vanishes at cryogenic temperatures, which corresponds to a low viscosity of a lubricant and, accordingly, a very weak energy dissipation. In the English-language scientific literature, this mode was coined as "superlubricity" [40, 41]. Let us examine the dependences of the friction force and the stresses for three types of lubricants – however, not on the temperature (as in Fig. 7), but on the proportionality coefficient k between the viscosity and the velocity gradient (see Eq. (7)). The corresponding plots are depicted in Fig. 8. Note that, in contrast to Fig. 7, different k-values correspond to different lubricants, friction surfaces, or experimental geometries. This means that every point in the dependences exhibited in Fig. 8 corresponds to tribological systems different by their properties. As one can see, for pseudoplastic fluids ($\gamma = -2/3$), the elastic stresses

remain constant with increase of the coefficient k. For Newtonian and dilatant fluids, the maximum stresses monotonously decrease with the increase of k. The friction force amplitude $F_{\max}$ grows with the coefficient k in the case of pseudoplastic fluid ($\gamma = -2/3$). At the same time, for the indices $\gamma = 0$ and $\gamma = 2/3$, the friction force behaves identically as in Fig. 7, i.e. it remains constant. However, within the whole presented range of k-values, $F_{\max}$ is minimal just for the pseudoplastic fluid; therefore, the latter is optimal for creating the conditions to reduce the friction in this case as well.

In Fig. 9, the behavior of the examined quantities is illustrated, as the spring stiffness constant K increases. For the dilatant and Newtonian fluids, the elastic stresses $\sigma_{\mathrm{el,max}}$ monotonously and slowly grow. In the case of the pseudoplastic fluid ($\gamma = -2/3$), the stresses drastically increase firstly, and afterward remain almost constant. The friction force in this case ($\gamma = -2/3$) also grows to a certain value and, then, does not almost change. For the indices $\gamma = 0$ and $\gamma = 2/3$, the amplitudes of friction force $F_{\max}$ linearly increase with the spring stiffness constant K, and their magnitudes are equal as in the previous two figures. Hence, in this case, the pseudoplastic fluid also provides the minimum friction force in the system. Thus, a general conclusion can be drawn that the pseudoplastic fluids provide an optimal friction mode in the tribological system exhibited in Fig. 1, because the maximum friction force $F_{\max}$ is the lowest for them.

6. Conclusions

In this work, a thermodynamic model was developed to describe the behavior of a tribological system functioning in the boundary friction mode. The model allowed a number of effects observed experimentally to be explained. It was shown that the stick-slip mode of motion is a result of the phase transition of the first order between the liquid- and solid-like states of a lubricant. The influence of the lubricant temperature, the spring stiffness constant, and the coefficient of proportionality between the viscosity and the velocity gradient on the system behavior was analyzed. For pseudoplastic fluids, the elastic stresses and the friction force were found to decrease with the temperature growth. The increase of the spring stiffness constant induces the growth of the friction force and stresses for all types of lubricants. When the coefficient of proportionality k increases, the maximum stresses do not change substantially in the case of pseudoplastic fluids, whereas the friction force grows. For the sake of comparison, the results of calculations obtained for the dilatant and Newtonian fluids were also reported. Modes, in which the displacement between the friction surfaces does not correspond to the direction of motion of the upper block, were revealed, which evidences the presence of memory effects in the system. While developing the model, the thermodynamic potential with two stable stationary states was used, in which the zero and nonzero minima were separated by a maximum. However, it was found experimentally that the lubricant is characterized by more than one type of transition and it can exist in a few (solid- or liquid-like) metastable states. For such a situation to be described, the additional terms of higher orders in the free energy expansion are sufficient to be taken into account.

I.A. Lyashenko is grateful to Prof. B.N.J. Persson for his invitation to make a research visit to the Forschungszentrum (Jülich, Germany), with this work being partially fulfilled there. He also thanks the organizers of the Joint ICTP-FANAS Conference on Trends in Nanotribology (September 12–16, 2011, Miramare, Trieste, Italy) for their invitation and financial support, as well as to A.E. Filippov and V.N. Samoilov for the discussion of this work at the indicated conference.

The work was supported by the the Ministry of Education and Science, Youth and Sport of Ukraine in the framework of the project "Modeling of friction for metal nanoparticles and boundary liquid films interacting with atomically smooth surfaces" (N 0112U001380).

1. B.N.J. Persson, *Sliding Friction. Physical Principles and Applications* (Springer, Berlin, 2000).
2. V.L. Popov, *Kontaktmechanik und Reibung. Ein Lehr- und Anwendungsbuch von der Nanotribologie bis zur numerischen Simulation* (Springer, Berlin, 2009).
3. J. Israelachvili, Surf. Sci. Rep. **14**, 109 (1992).
4. J. Ringlein and M.O. Robbins, Am. J. Phys. **72**, 884 (2004).
5. H. Yoshizawa and J. Israelachvili, J. Phys. Chem. **97**, 11300 (1993).
6. A.D. Berman, W.A. Ducker, and I.N. Israelachvili, Langmuir **12**, 4559 (1996).
7. V.L. Popov, Tech. Phys. **46**, 605 (2001).
8. I.A. Lyashenko, A.V. Khomenko, and L.S. Metlov, Tech. Phys. **55**, 1193 (2010).
9. A.E. Filippov, J. Klafter, and M. Urbakh, Phys. Rev. Lett. **92**, 135503 (2004).

10. J.M. Carlson and A.A. Batista, Phys. Rev. E **53**, 4153 (1996).
11. A.V. Khomenko and I.A. Lyashenko, J. Phys. Studies **11**, 268 (2007).
12. A.V. Khomenko and I.A. Lyashenko, Tech. Phys. **52**, 1239 (2007).
13. A.V. Khomenko, I.A. Lyashenko, and V.N. Borisyuk, Ukr J. Phys. **54**, 1139 (2009).
14. A.V. Khomenko, I.A. Lyashenko, and V.N. Borisyuk, Fluct. Noise Lett. **9**, 19 (2010).
15. A.L. Demirel and S. Granick, J. Chem. Phys. **109**, 6889 (1998).
16. G. Reiter, A.L. Demirel, J. Peanasky, L.L. Cai, and S. Granick, J. Chem. Phys. **101**, 2606 (1994).
17. A.V. Khomenko and I.A. Lyashenko, Phys. Sol. State **49**, 936 (2007).
18. A.V. Khomenko and I.A. Lyashenko, Tech. Phys. **55**, 26 (2010).
19. A.V. Khomenko and I.A. Lyashenko, Journal of Friction and Wear**31**, 308 (2010).
20. V.L. Popov, Solid State Commun. **115**, 369 (2000).
21. L.D. Landau and E.M. Lifshits, *Statistical Physics, Part 1* (Pergamon Press, Oxford, 1980).
22. A. Lemaître and J. Carlson, Phys. Rev. E **69**, 061611 (2004).
23. A. Lemaître, Phys. Rev. Lett. **89**, 195503 (2002).
24. J.N. Israelachvili, *Intermolecular and Surface Forces: With Applications to Colloidal and Biological Systems* (Academic Press, New York, 1991).
25. J.N. Israelachvili, Chemtracts Analyt. Phys. Chem. **1**, 1 (1989).
26. C.-R. Yang, Y.-C. Chiou, and R.-T. Lee, Tribol. Int. **32**, 443 (1999).
27. C.-R. Yang, R.-T. Lee, Y.-C. Chiou, Tribol. Int. **30**, 719 (1997).
28. G. Luengo, J. Israelachvili, and S. Granick, Wear **200**, 328 (1996).
29. I.M. Sivebaek, V.N. Samoilov, and B.N.J. Persson, Phys. Rev. Lett. **108**, 036102 (2012).
30. I.A. Lyashenko, Tech. Phys. **56**, 869 (2011).
31. I.A. Lyashenko, Tech. Phys. **57**, 17 (2012).
32. I.A. Lyashenko, A.V. Khomenko, and L.S. Metlov, Ukr. J. Phys. **56**, 278 (2011).
33. I.A. Lyashenko, A.V. Khomenko, and L.S. Metlov, Tribol. Int. **44**, 476 (2011).
34. V.L. Popov, Tech. Phys. Lett. **25**, 815 (1999).
35. A.I. Olemskoi, Physica A **310**, 223 (2002).
36. O.M. Braun, N. Manini, and E. Tosatti, Phys. Rev. B **78**, 195402 (2008).
37. I.S. Aranson, L.S. Tsimring, and V.M. Vinokur, Phys. Rev. B **65**, 125402 (2002).
38. L.D. Landau and I.M. Khalatnikov, Dokl. Akad. Nauk SSSR **96**, 469 (1954).
39. I.A. Lyashenko, Tech. Phys. **56**, 701 (2011).
40. A.E. Filippov, M. Dienwiebel, J.W.M. Frenken, J. Klafter, and M. Urbakh, Phys. Rev. Lett. **100**, 046102 (2008).
41. M. Hirano, Wear **254**, 932 (2003)

Received 20.03.12.
Translated from Ukrainian by O.I. Voitenko

Я.О. Ляшенко, А.М. Заскока

ПЕРЕРИВЧАСТИЙ РЕЖИМ МЕЖОВОГО ТЕРТЯ ЯК ФАЗОВИЙ ПЕРЕХІД ПЕРШОГО РОДУ

Р е з ю м е

Розглянуто трибологічну систему, що складається з двох контактуючих блоків, один з яких закріплений між двома пружинами, а інший приведений в неперервний періодичний рух. Досліджено кінетику системи в режимі межового тертя, коли між атомарно-гладкими поверхнями блоків знаходиться ультратонка плівка мастила. Для опису стану мастила записано вираз для густини вільної енергії у вигляді розкладання в ряд за степенями параметра порядку, який зводиться до модуля зсуву. Показано, що в широкому діапазоні параметрів реалізується переривчастий режим руху, до якого приводять періодичні фазові переходи першого роду між кінетичними режимами тертя. Спрогнозовано поведінку системи при зміні зовнішніх та внутрішніх параметрів.